

# Transmission from stable to stable radiation through self-modulation and chaotic oscillations in multiwave Cherenkov generator

*V.I. Koshelev\**, *V.A. Chazov*, *A.A. Petkun*

*Institute of High Current Electronics SB RAS, Tomsk, Russia*

*\*koshelev@lhfe.hcei.tsc.ru*

**Abstract.** A numerical simulation of a multiwave Cherenkov generator with a diffraction reflector in the subterahertz (112–114 GHz) frequency range has been performed using a 2.5D hybrid electromagnetic PIC code. A tubular beam with an electron energy of 180–490 keV and a current of 1–30 kA was injected into an electrodynamic system with a diameter of 36.4 mm. Two regimes were found in numerical experiments. With an electron energy near 280 keV, a high (88%) efficiency of bringing radiation power forward was obtained. With an electron energy near 250 keV, a power self-modulation regime was found. In the multiwave Cherenkov generator, for the first time, a transition was found from stable generation at a power of 6.8 MW to stable generation at a power of 800 MW through self-modulation and chaotic power oscillations with an increase in beam current. In this case, the ratio of the beam current to the starting generation current varied from 1.3 to 16.7.

**Keywords:** multiwave Cherenkov generator, subterahertz radiation, self-modulation.

## 1. Introduction

Currently, active research is underway to generate powerful radiation in the subterahertz (100–300 GHz) frequency range. Radiation pulses with a power of 50–70 MW at a frequency near 140 GHz were obtained in a vacuum electronic device based on a surface wave oscillator [1]. The ratio of the diameter to the wavelength of the radiation  $D/\lambda = 3.5$ . A flat reflector was used at the entrance of the slow-wave structure.

Sectioning the oversized slow-wave structure makes it possible to use surface and bulk waves and increase the efficiency of radiation generation. This approach is used in a multiwave Cherenkov generator (MWCG). On the SINUS-7M accelerator with a voltage pulse duration of 40 ns, studies of MWCG [2] with  $D/\lambda = 13.3$  ( $D = 118$  mm,  $\lambda = 8.84$  mm) were performed. There was no reflector at the input of the two-section slow-wave structure. In the experiments, radiation pulses with a power of 500–600 MW were obtained. The fraction of axially symmetric radiation power was 90%. The width of the radiation spectrum was no more than 0.5%. The cross-sectional geometry of the tubular electron beam was elliptical. This was due to the design of the solenoid. The difference between the major and minor axes of the ellipse was less than 1 mm.

The purpose of this work is the numerical simulation of MWCG with  $D/\lambda = 13.6$  in the subterahertz (112–114 GHz) frequency range. A diffraction reflector is used to increase the fraction of forward radiation power. Special attention in numerical experiments is paid to the power self-modulation regime, which was previously discovered [3] and studied in detail [4] in terahertz (358–368 GHz) MWCG.

## 2. Numerical simulation of MWCG

A 2.5D hybrid electromagnetic PIC code was used for numerical simulation of MWCG without taking into account ohmic power losses [5, 6]. A tubular beam with electron energy  $W_e = 180$ –490 keV, current  $I_b = 1$ –30 kA, middle radius  $r_b = 16.9$ –17.5 mm and thickness 0.5 mm was injected into an electrodynamic system with a radius of 18.2 mm with pre-calculated fields of longitudinal electromagnetic resonances. The duration of the leading edge of the beam current pulse  $I_b$  and, accordingly, the diode voltage  $U_d$  was 0.5 ns. The magnetic field varied within  $B = 1$ –5 T. The electrodynamic system contains a diffraction reflector with 6 diaphragms and two sections of a periodic waveguide with 18 and 12 diaphragms. The distance between the diffraction reflector and the first section  $L_r = 0.8$  mm was constant. The length of the drift tube between the sections of the

slow-wave structure varied within the range of  $L_{dr} = 1.32\text{--}2.6$  mm. The rectangular diaphragms had a width of 0.54 mm and a height of 0.35 mm. The diaphragms periods in the diffraction reflector and sections of the slow-wave structure are 1.3 mm and 1 mm, respectively.

The calculations took into account the first three longitudinal resonances  $R_n$  ( $n = 1, 2, 3$ ), calculated from the frequency of  $\pi$ -type oscillations of the  $TM_{01}$  mode (114.7 GHz) of an infinite periodic ( $d = 1$  mm) waveguide, which corresponds to an electron energy near 280 keV. Resonances are characterized by frequency  $F$ ,  $Q$  factor,  $N_e$  norm and field structure. The calculations estimated the forward ( $P^+$ ), backward ( $P^-$ ) and total power ( $P^- + P^+$ ) radiation. To analyze the interaction of the beam and the field, the resonance amplitudes, the synchronization frequency  $f_s$ , the instantaneous frequencies  $f_i$ , resonance spectra  $S_i$ , and the frequency of the maximum of the spectrum  $f_0$  were estimated. The radiation spectrum  $S(f)$  was also calculated. The parameters of the radiation power are given after the generation goes into stationary regime. The geometry of an electrodynamic system with an electron beam ( $W_e = 250$  keV,  $I_b = 5$  kA,  $B = 3$  T,  $r_b = 17$  mm,  $L_{dr} = 2.0$  mm) for the time  $t = 5$  ns is shown in Fig. 1.

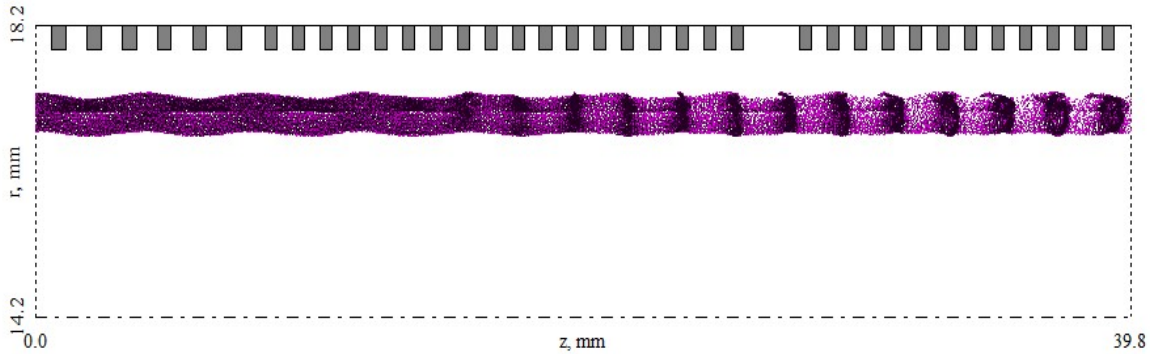


Fig. 1. The geometry of the MWCG electrodynamic system with a beam ( $W_e = 250$  keV,  $I_b = 5$  kA,  $B = 3$  T,  $r_b = 17$  mm,  $L_{dr} = 2.0$  mm) at time  $t = 5$  ns.

Figures 2a, 2b show the dependences of the forward  $P^+$  radiation power and the  $P^+/P$  ratio on the average values at the electron energy in the range  $W_e = 220\text{--}380$  keV for three values  $L_{dr} = 1.32, 2.0, 2.6$  mm with beam parameters  $I_b = 5$  kA,  $B = 3$  T,  $r_b = 17$  mm. At an electron energy of less than 220 keV, the radiation power decreased sharply. With an electron energy of more than 380 keV, the  $P^+/P$  ratio was low and constant.

Initially, we will consider the characteristics of radiation near the energy  $W_e = 280$  keV and  $L_{dr} = 2.6$  mm. The total radiation power is  $P = 52$  MW (Fig. 2a). The ratio of  $P^+/P = 88\%$  (Fig. 2b). The starting generation current at the above parameters is  $I_{st} = 3$  kA. The maximum generation efficiency corresponds to  $I_b = 4\text{--}5$  kA. The radiation power after resonance synchronization is stable and increases to  $P = 172$  MW at  $P^+/P = 63\%$  with an increase in the beam current up to 25 kA. The  $I_b/I_{st}$  ratio reaches 8.3 with stable radiation generation. With an increase in the beam current  $I_b = 3\text{--}25$  kA, the frequency of synchronized resonances varies between 112.9–113.4 GHz. The maximum frequency corresponds to  $I_b = 15$  kA. The radiation spectrum is narrow. The maximum of the spectrum  $f_0$  practically coincides with the frequency of synchronization of electromagnetic resonances  $f_s$ . With stable radiation generation, the average power value  $\langle P \rangle$  corresponds to the power in stationary regime.

A power self-modulation regime was detected in the electron energy range  $W_e = 245\text{--}260$  keV and  $L_{dr} = 2.0$  mm (Fig. 2a). To estimate the depth of self-modulation of the total radiation power, we use the coefficient  $k_{sm} = (P_{max} - P_{min})/P_{max}$ . A similar coefficient  $k_{sm}^+$  and  $k_{sm}^-$  is used to estimate the depth of self-modulation of the radiation power forward  $P^+$  and backward  $P^-$ .

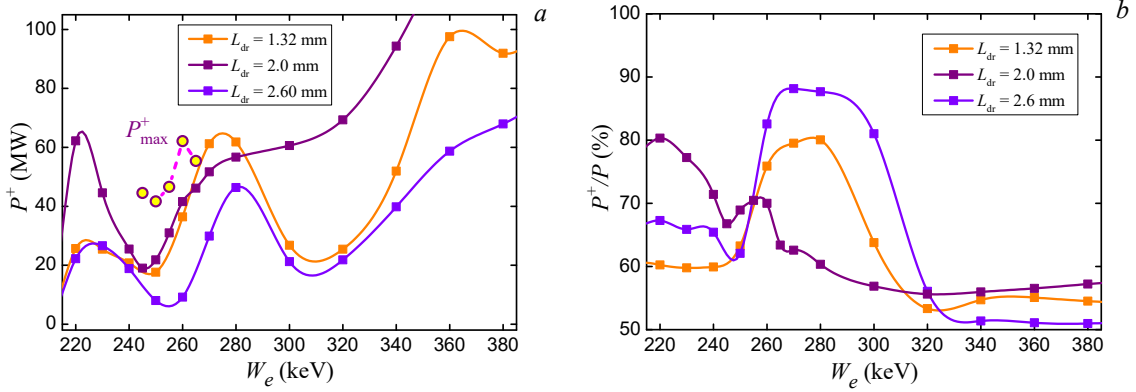


Fig. 2. The forward radiation power (a) and the  $P^+/P$  ratio (b) versus the electron energy of the beam (5 kA, 3 T, 17 mm) for different drift tube lengths.

The starting generation current  $I_{st} = 1.5$  kA at an energy of  $W_e = 250$  keV,  $r_b = 17$  mm and  $B = 3$  T. Figure 3a,b shows the results of numerical experiments for a beam with parameters  $I_b = 5$  kA,  $r_b = 17$  mm and  $B = 3$  T in the electron energy range  $W_e = 240$ –270 keV. The upper and lower curves correspond to  $P^+_{max}$  and  $P^+_{min}$ . Hereafter  $\langle P \rangle$  corresponds to the average power value. The maximum forward power modulation depth  $k_{sm}^+ = 87\%$  was obtained at  $W_e = 250$  keV. In the subsequent calculations, we chose the value  $W_e = 250$  keV.

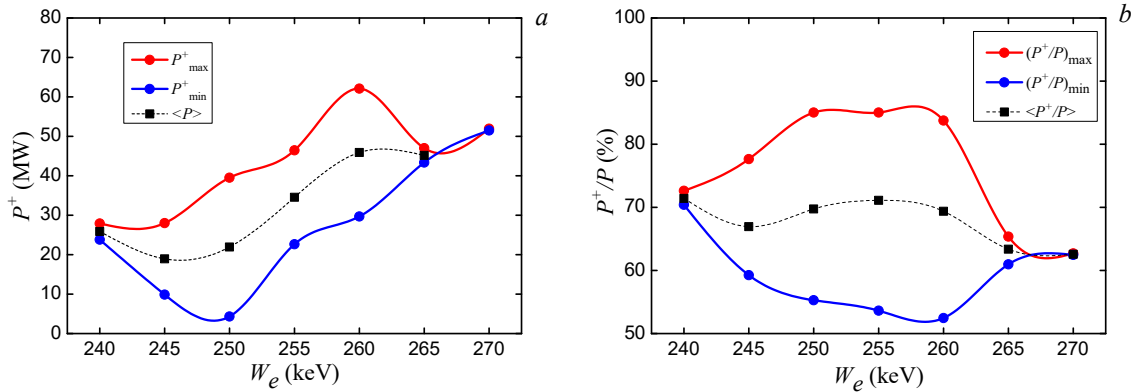


Fig. 3. The forward radiation power (a) and the  $P^+/P$  ratio (b) versus the electron energy in the self-modulation regime.

Figure 4a shows the results of numerical experiments for a beam with parameters  $W_e = 250$  keV,  $I_b = 5$  kA and  $B = 3$  T with a change in the beam radius within 16.9–17.5 mm. The upper and lower curves correspond to  $P_{max}$  and  $P_{min}$ . Self-modulation of power was detected in a narrow range of beam radius  $r_b = 17.0$ –17.2 mm. The maximum modulation depth  $k_{sm} = 92.6\%$  was obtained at  $r_b = 17.1$  mm. For further calculations, we chose the value  $r_b = 17$  mm in order to move the beam away from the surface of the electrodynamic system.

The results of numerical experiments with variations in the magnetic field in the range  $B = 1$ –5 T, beam current  $I_b = 5$  kA and other similar parameters are shown in Fig. 4b. There was no self-modulation of the radiation power at  $B = 1$  T. Power oscillations were damped in a magnetic field  $B = 1.25$  T with a beam current pulse duration of more than 25 ns. The main calculations were carried out at the beam current pulse duration  $\tau_b = 25$ –30 ns, and special calculations for  $I_b = 13$  kA were carried out at  $\tau_b = 70$  ns. Regular self-modulation of power occurs in a magnetic field  $B = 1.5$  T. The amplitude of the self-modulation of power increases with an increase in the magnetic field to  $B = 2$  T and then remains approximately constant up to  $B = 5$  T. For subsequent calculations, we chose the value  $B = 3$  T.

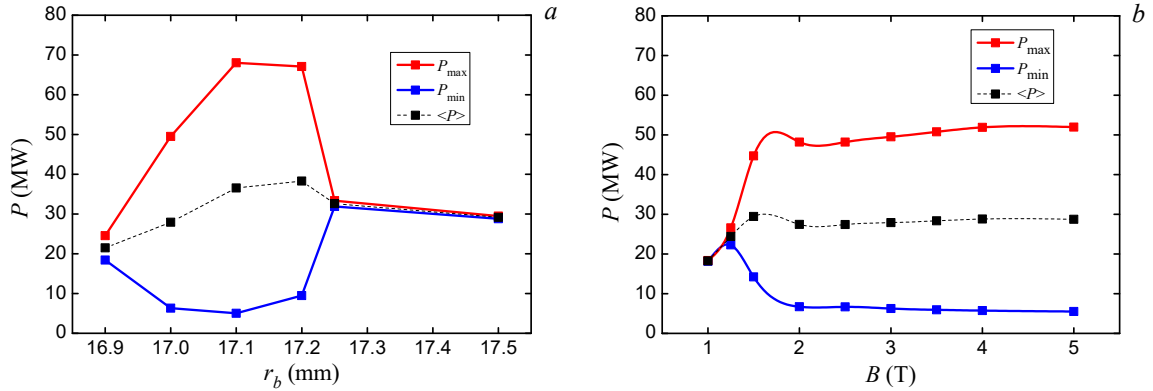


Fig. 4. The dependence of the total radiation power versus the beam radius (a) and the magnetic field (b).

The most interesting are the results of numerical studies of the effect of beam current on radiation generation regimes. Figure 5a,b shows the dependences of the total radiation power and the  $P^+/P$  ratio versus the beam current. Figure 6 shows the dependences of the forward  $k_{sm}^+$  and backward  $k_{sm}^-$  power modulation coefficients, as well as the waveforms of the total radiation power in a wide range of beam current  $I_b = 1.5$ –25 kA for different generation regimes.

The radiation power is stable at a beam current  $I_b = 1.5$ –2 kA. Damping oscillations are observed at a beam current  $I_b = 2.5$ –3 kA. Regular power oscillations in stationary regime occur when the beam current increases to  $I_b = 3.5$  kA. At the same time, the ratio  $I_b/I_{st} = 2.3$ . The depth of regular self-modulation of the total power increases from 56% to 93% with an increase in the beam current within  $I_b = 3.5$ –8.5 kA. The total oscillation power reaches 126 MW. The frequency of regular self-modulation of power varied between 0.6–0.8 GHz. When the beam current is  $I_b = 9$ –13 kA, power oscillations become irregular (chaotic). With an increase in the beam current to 14 kA, a sudden transition from chaotic power oscillations to regular power oscillations occurred. With a further increase in the beam current to  $I_b = 15$ –25 kA, power oscillations damped. A stable radiation generation regime was obtained at a beam current  $I_b = 25$  kA. The ratio  $I_b/I_{st} = 16.7$  corresponds to this current. When the beam current is increased to  $I_b = 30$  kA, the stable radiation generation regime is maintained.

Thus, we observed a complex transition from stable power generation to stable power generation through a sequence of damped, regular, chaotic, regular, damped oscillations.

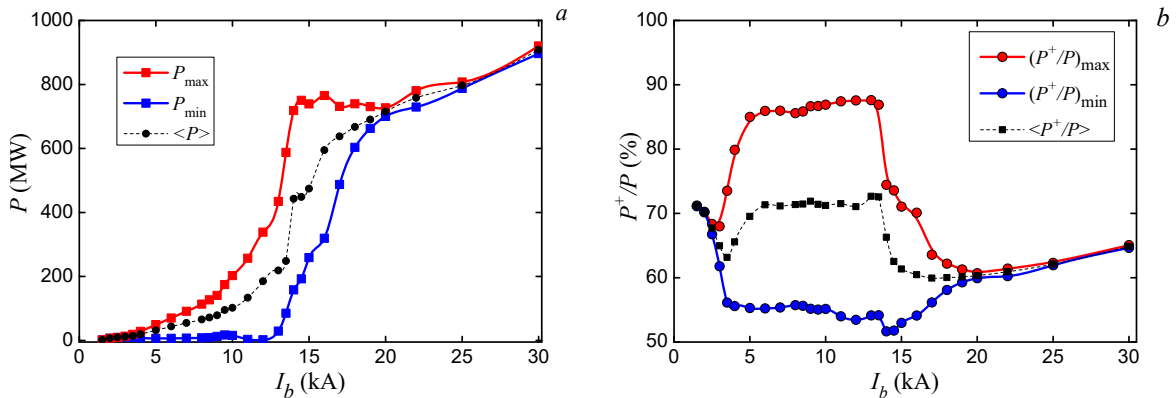


Fig. 5. The total radiation power (a) and the  $P^+/P$  ratio (b) versus the beam current.

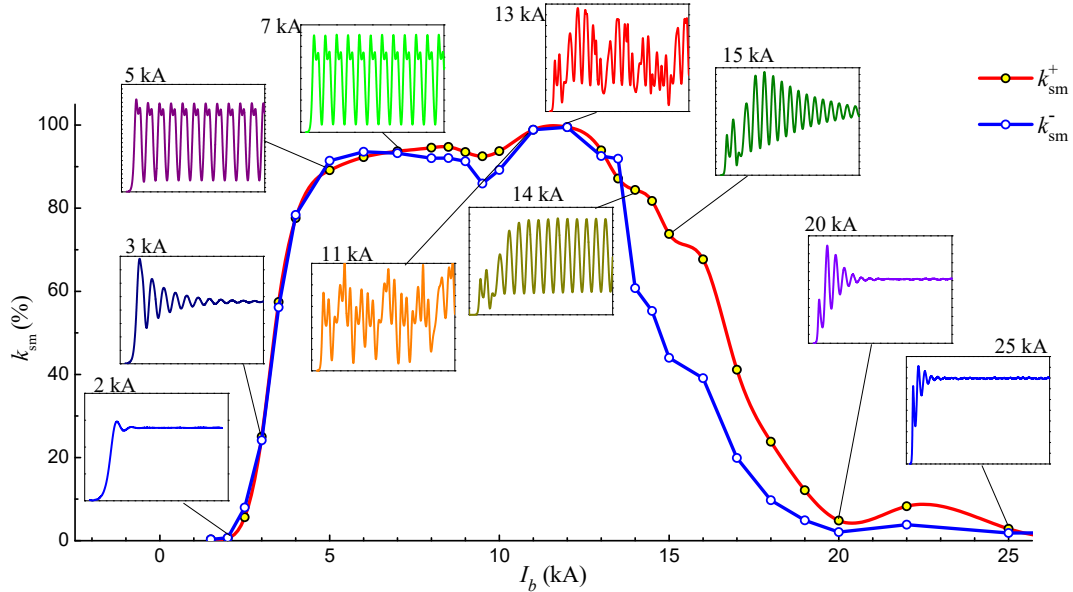


Fig. 6. The coefficients of self-modulation of forward and backward power and waveforms of the total radiation power for different beam currents.

Figure 7 shows the radiation spectra at the MWCG output for different generation regimes at a beam current of 5 kA, 13 kA and 25 kA. With regular self-modulation of power (5 kA), the radiation spectrum consists of several narrow frequency bands. With irregular (chaotic) power oscillation (13 kA), the spectrum expands. With stable power generation (25 kA), the radiation spectrum is narrow.

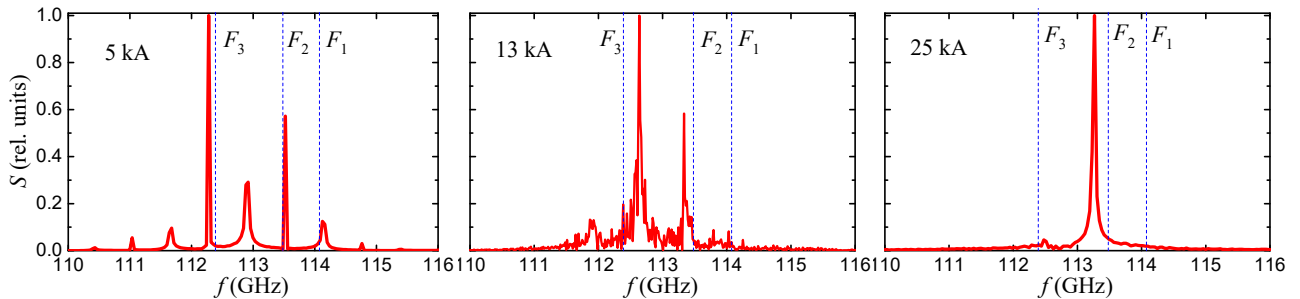


Fig. 7. The field oscillation spectra for different generation regimes at a beam current of 5 kA, 13 kA and 25 kA.

### 3. Conclusion

The self-modulating power generation regime was obtained at a ratio of  $I_b/I_{st} = 2.3$  and electron energy near 250 keV. With a ratio of  $I_b/I_{st} = 8.3$  and an electron energy of 280 keV, which corresponds to the  $\pi$ -type oscillations of the  $TM_{01}$  mode of an infinite periodic waveguide, there was no self-modulation of power. These results are consistent with the conclusions of theoretical studies of the Cherenkov generator near the high-frequency transmission band boundary of the  $TM_{01}$  mode [7]. The authors [7] showed that the  $I_b/I_{st}$  ratio for the power self-modulation regime in a homogeneous slow-wave structure near the  $\pi$ -type oscillations of the  $TM_{01}$  mode is much higher than for the backward wave oscillator. However, in our previous studies of terahertz MWCG [3, 4], deep self-modulation of power was obtained at an electron energy of 420 keV ( $L_{dr} = 2.4\text{--}3.6$  mm,  $\lambda = 0.82$  mm) corresponding to the  $\pi$ -type oscillations of the  $TM_{01}$  mode of an infinite periodic waveguide.

The sectioning of the slow-wave structure in the MWCG affects the ratio of the amplitudes of the longitudinal electromagnetic resonances and, accordingly, the beam parameters, at which the

transition from stable radiation generation to the power self-modulation regime occurs. The transition from irregular (chaotic) oscillations to stable power generation with increasing beam current is due to the influence of the spatial charge of the beam on the synchronization of longitudinal electromagnetic resonances.

### Acknowledgement

This work was supported by the Ministry of Science and Higher Education of the Russian Federation (project no. FWRM-2021-0002).

### 4. References

- [1] N.S. Ginzburg, A.M. Malkin, A.S. Sergeev, I.V. Zheleznov, I.V. Zotova, V.Yu Zaslavsky., G.Sh. Boltachev, K.A. Sharypov, S.A. Shunailov, M.R. Ul'masculov, and M.I. Yalandin, Generation of subterahertz superradiance pulses based on excitation of a relativistic electron bunches moving in oversized corrugated waveguides, *Phys. Rev. Lett.*, vol. **117**, 204801, 2016, doi: 10.1103/PhysRevLett.117.204801
- [2] V.I. Koshelev, V.A. Popov, Relativistic multiwave Cerenkov generators of millimeter wavelength range, *Proc. SPIE*, vol. **4031**, 270, 2000, doi: 10.1117/12.391808
- [3] V.A. Chazov, M.P. Deichuly, V.I. Koshelev, and A.A. Petkun, Interaction between electron beam and electromagnetic field in terahertz multiwave Cherenkov generator with diffraction reflector, *Russian Physics Journal*, vol. **66**, 567, 2023, doi: 10.1007/s11182-023-02976-3
- [4] V.A. Chazov, M.P. Deichuly, V.I. Koshelev, and A.A. Petkun, A study of the influence of the beam and field parameters on the terahertz multiwave Cherenkov generator efficiency, *Russian Physics Journal*, vol. **67**, 102, 2024, doi: 10.1007/s11182-024-03094-4
- [5] M.P. Deichuly, V.I. Koshelev, A.A. Petkun, V.A. Chazov, Synchronization of electromagnetic resonances in terahertz Cherenkov generator, *Izvestiya vuzov. Fizika*, vol. **66**, 92, 2023, doi: 10.17223/00213411/66/6/11
- [6] M.P. Deichuly, V.I. Koshelev, A.A. Petkun, and V.A. Chazov, Interaction of a relativistic electron beam and electromagnetic field in a terahertz Cherenkov generator with a Bragg reflector, *Journal of Commun. Technol. Electronics*, vol. **68**, 1430, 2023, doi: 10.1134/S1064226923120057
- [7] L.V. Bulgakova, S.P. Kuznetsov, Unsteady-state nonlinear processes accompanying the interaction of an electron beam with an electromagnetic field near the boundary of a transmission band. 1. The high-frequency boundary, *Radiophysics and Quantum Electronics*, vol. **31**, 155, 1988, doi: 10.1007/BF01039179